
On the distance between two neural networks and the stability of learning

Jeremy Bernstein
Caltech

bernstein@caltech.edu

Arash Vahdat
NVIDIA

avahdat@nvidia.com

Yisong Yue
Caltech

yyue@caltech.edu

Ming-Yu Liu
NVIDIA

mingyul@nvidia.com

Abstract

This paper relates *parameter distance* to *gradient breakdown* for a broad class of nonlinear compositional functions. The analysis leads to a new distance function called *deep relative trust* and a descent lemma for neural networks. Since the resulting learning rule seems not to require learning rate grid search, it may unlock a simpler workflow for training deeper and more complex neural networks. Please find the Python code used in this paper here: <https://github.com/jxbz/fromage>.

1 Introduction

Gradient descent is the workhorse of deep learning. To decrease a loss function $\mathcal{L}(W)$, this simple algorithm pushes the neural network parameters W along the negative gradient of the loss. One motivation for this rule is that it minimises the local loss surface under a quadratic trust region [1]:

$$\underbrace{W - \eta \nabla \mathcal{L}(W)}_{\text{gradient descent}} = W + \arg \min_{\Delta W} \left[\underbrace{\mathcal{L}(W) + \nabla \mathcal{L}(W)^T \Delta W}_{\text{local loss surface}} + \underbrace{\frac{1}{2\eta} \|\Delta W\|_2^2}_{\text{quadratic penalty}} \right]. \quad (1)$$

Since a quadratic trust region does not capture the compositional structure of a neural network, it is difficult to choose the learning rate η in practice. Goodfellow et al. [2, p. 424] advise:

If you have time to tune only one hyperparameter, tune the learning rate.

Practitioners usually resort to tuning η over a logarithmic grid. If that fails, they may try tuning a different optimisation algorithm such as Adam [3]. But the cost of grid search scales exponentially in the number of interacting neural networks, and state of the art techniques involving just two neural networks are difficult to tune [4] and often unstable [5]. Eliminating the need for learning rate grid search could enable new applications involving multiple competitive and/or cooperative networks.

With that goal in mind, this paper replaces the quadratic penalty appearing in Equation 1 with a novel distance function tailored to the compositional structure of deep neural networks.

Our contributions:

1. By a direct perturbation analysis of the neural network function and Jacobian, we derive a distance on neural networks called *deep relative trust*.
2. We show how to combine deep relative trust with the fundamental theorem of calculus to derive a descent lemma tailored to neural networks.
3. From the new descent lemma, we derive a learning algorithm that we call Frobenius matched gradient descent—or *Fromage*. Fromage has only one hyperparameter with a clear meaning.
4. We show that, *with no learning rate tuning*, Fromage works well across a range of standard neural network benchmarks including generative adversarial networks, natural language transformers, and image classifiers.

2 Entendámonos...

...so we understand each other.

The goal of this section is to review a few basics of deep learning, including heuristics commonly used in algorithm design and areas where current optimisation theory falls short. We shall see that a good notion of distance between neural networks is still a subject of active research.

Deep learning basics

Deep learning seeks to fit a *neural network* function $f(W; x)$ with parameters W to a dataset of N input-output pairs $\{x_i, y_i\}_{i=1}^N$. If we let $\mathcal{L}_i := \mathcal{L}(f_i, y_i)$ measure the discrepancy between prediction $f_i := f(W; x_i)$ and target y_i , then learning proceeds by gradient descent on the *loss*: $\sum_{i=1}^N \mathcal{L}_i$.

Though various neural network architectures exist, we shall focus our theoretical effort on the *multilayer perceptron*, which already contains the most striking features of general neural networks: matrices, nonlinearities, and layers.

Definition 1 (Multilayer perceptron). A multilayer perceptron is a function $f : \mathbb{R}^{n_0} \rightarrow \mathbb{R}^{n_L}$ composed of L layers. The l th layer is a linear map $W_l : \mathbb{R}^{n_{l-1}} \rightarrow \mathbb{R}^{n_l}$ followed by a nonlinearity $\varphi : \mathbb{R} \rightarrow \mathbb{R}$ that is applied elementwise. We may describe the network in two complementary ways:

$$f(x) := \underbrace{\varphi \circ W_L}_{\text{layer } L} \circ \underbrace{\varphi \circ W_{L-1}}_{\text{layer } L-1} \circ \dots \circ \underbrace{\varphi \circ W_1}_{\text{layer } 1}(x); \quad (L \text{ layer network})$$

$$h_l(x) := \varphi(W_l h_{l-1}(x)); \quad h_0(x) := x. \quad (\text{hidden layer recursion})$$

Since we wish to fit the network via gradient descent, we shall be interested in the gradient of the loss with respect to the l th parameter matrix. This may be decomposed via the chain rule. Schematically:

$$\nabla_{W_l} \mathcal{L} = \frac{\partial \mathcal{L}}{\partial f} \cdot \frac{\partial f}{\partial h_l} \cdot \varphi'(W_l h_{l-1}) \cdot h_{l-1}. \quad (2)$$

The famous backpropagation algorithm [6] observes that the second term may be decomposed over the layers of the network. Following the notation of Pennington et al. [7]:

Proposition 1 (Jacobian of the multilayer perceptron). Consider a multilayer perceptron with L layers. The layer- l -to-output Jacobian J_l is given by:

$$J_l := \frac{\partial f(x)}{\partial h_l} = \frac{\partial f}{\partial h_{L-1}} \cdot \frac{\partial h_{L-1}}{\partial h_{L-2}} \cdot \dots \cdot \frac{\partial h_{L-1}}{\partial h_l}$$

$$= \Phi'_L W_L \cdot \Phi'_{L-1} W_{L-1} \cdot \dots \cdot \Phi'_{l+1} W_{l+1},$$

where $\Phi'_k := \text{diag}[\varphi'(W_k h_{k-1}(x))]$ denotes the derivative of the nonlinearity at the k th layer.

A key observation is that the network function f and Jacobian $\frac{\partial f}{\partial h_l}$ share a common mathematical structure—a deep, layered composition. We shall exploit this in our theory.

Empirical deep learning

The formulation of gradient descent given in Equation 1 quickly encounters a problem known as the *vanishing and exploding gradient problem*, where the scale of updates becomes miscalibrated with the scale of parameters in different layers of the network. Common tricks to ameliorate the problem include careful choice of weight initialisation [8], dividing out the gradient scale [3], gradient clipping [9] and directly controlling the relative size of updates to each layer [10, 11]. Each of these techniques has been adopted in numerous deep learning applications.

Still, there is a cost to using heuristic techniques. For instance, techniques that rely on careful initialisation may break down by the end of training, leading to instabilities that are difficult to trace. These heuristics also lead to a proliferation of hyperparameters that are difficult to interpret and tune. We may wonder, *why does our optimisation theory not handle these matters for us?*

Deep learning optimisation theory

It is common in optimisation theory to assume that the loss has Lipschitz continuous gradients:

$$\|\nabla\mathcal{L}(W + \Delta W) - \nabla\mathcal{L}(W)\|_2 \leq \frac{1}{\eta}\|\Delta W\|_2.$$

By a standard argument involving the quadratic penalty mentioned in the introduction, this assumption leads to gradient descent [1]. This assumption is ubiquitous to the point that it is often just referred to as *smoothness* [12]. It is used in a number of works in the context of deep learning optimisation [12–15], distributed training [16], and generative adversarial networks [17].

We conduct an empirical study that shows that neural networks do not have Lipschitz continuous gradients in practice. We do this for a 16 layer multilayer perceptron (Figure 1), and find that the gradient grows roughly exponentially in the size of a perturbation. See [18] for more empirical investigation, and [19] for more discussion on this point.

Several classical optimisation frameworks go beyond the quadratic penalty $\|\Delta W\|_2^2$ of Equation 1:

1. Mirror descent [20] replaces $\|\Delta W\|_2^2$ by a *Bregman divergence* appropriate to the geometry of the problem. This framework was studied in relation to deep learning [21, 22], but it is still unclear whether there is a Bregman divergence that models the compositional structure of neural networks.
2. Natural gradient descent [23] replaces $\|\Delta W\|_2^2$ by $\Delta W^T F \Delta W$. The *Riemannian metric* $F \in \mathbb{R}^{d \times d}$ should capture the geometry of the d -dimensional function class. Unfortunately, even writing down a $d \times d$ matrix is intractable for modern neural networks. Whilst some works explore tractable approximations [24], natural gradient descent is still a quadratic model of trust—we find that trust is lost far more catastrophically in deep networks.
3. Steepest descent [25] replaces $\|\Delta W\|_2^2$ by an arbitrary distance function. Neyshabur et al. [26] explore this approach using a rescaling invariant norm on paths through the network. The downside to the freedom of steepest descent is that it does not operate from first principles—so the chosen distance function may not match up to the problem at hand.

Other work operates outside of these frameworks. Several papers study the effect of architectural decisions on signal propagation through the network [7, 27–30], though these works usually neglect functional distance and curvature of the loss surface. Pennington and Bahri [31] do study curvature of the loss surface, but rely on random matrix models to make progress.

Generative adversarial networks

Neural networks can learn to generate samples from complex distributions. Generative adversarial learning [32] trains a discriminator network D to classify data as real or fake, and a generator network G is trained to fool D . Competition drives learning in both networks. Letting \mathcal{V} denote the success rate of the discriminator, the learning process is described as:

$$\min_G \max_D \mathcal{V}(G, D).$$

Defining the optimal discriminator for a given generator as $D^*(G) := \arg \max_D \mathcal{V}(G, D)$. Then generative adversarial learning reduces to a straightforward minimisation over the parameters of the generator:

$$\min_G \max_D \mathcal{V}(G, D) \equiv \min_G \mathcal{V}(G, D^*(G)).$$

In practice this is solved as an inner-loop, outer-loop optimisation procedure where k steps of gradient descent are performed on the discriminator, followed by 1 step on the generator. For example, Miyato et al. [33] take $k = 5$ and Brock et al. [5] take $k = 2$.

For small k , this procedure is only well founded if the perturbation ΔG to the generator is small so as to induce a small perturbation in the optimal discriminator. In symbols, we hope that:

$$\|\Delta G\| \ll 1 \implies \|D^*(G + \Delta G) - D^*(G)\| \ll 1.$$

But what does $\|\Delta G\|$ mean? In what sense should it be small? We see that this is another area that could benefit from an appropriate notion of distance on neural networks.

3 The distance between networks

Suppose that a teacher wishes to assess a student’s learning. Traditionally, they will assign the student homework and track their progress. What if, instead, they could peer inside the student’s head and observe change directly in the synapses—would that not be better for everyone?

We would like to establish a meaningful notion of functional distance for neural networks. This should let us know how far we can safely perturb a network’s weights without needing to tune a learning rate and measure the effect on the loss empirically.

The quadratic penalty of Equation 1 is akin to assuming a Euclidean structure on the parameter space, where the squared Euclidean length of a parameter perturbation determines how fast the loss function breaks down. The main pitfall of this assumption is that it does not reflect the deep compositional structure of a neural network. We propose a new trust concept called *deep relative trust*. In this section, we shall motivate deep relative trust—the formal definition shall come in Section 4.

Deep relative trust will involve a product over relative perturbations to each layer of the network. For a first glimpse of how this structure arises, consider a simple network that multiplies its input $x \in \mathbb{R}$ by two scalars $a, b \in \mathbb{R}$. That is $f(x) = a \cdot b \cdot x$. Also consider perturbed function $\tilde{f}(x) = \tilde{a} \cdot \tilde{b} \cdot x$ where $\tilde{a} := a + \Delta a$ and $\tilde{b} := b + \Delta b$. Then the relative difference obeys:

$$\frac{|\tilde{f}(x) - f(x)|}{|f(x)|} \leq \left(1 + \frac{|\Delta a|}{|a|}\right) \left(1 + \frac{|\Delta b|}{|b|}\right) - 1. \quad (3)$$

The simple derivation may be found at the beginning of Appendix B. The key point is that the relative change in the composition of two operators depends on the product of the relative change in each operator. The same structure extends to the relative distance between two neural networks—both in terms of function and gradient—as we will now demonstrate.

Theorem 1. *Let f be a multilayer perceptron with nonlinearity φ and L weight matrices $\{W_l\}_{l=1}^L$. Let \tilde{f} be a second network with the same architecture but different weight matrices $\{\tilde{W}_l\}_{l=1}^L$. For convenience, define layerwise perturbation matrices $\{\Delta W_l := \tilde{W}_l - W_l\}_{l=1}^L$.*

Further suppose that the following two conditions hold:

1. *Transmission. There exist $\alpha, \beta \geq 0$ such that $\forall x, y$:*

$$\begin{aligned} \alpha \cdot \|x\|_2 &\leq \|\varphi(x)\|_2 \leq \beta \cdot \|x\|_2; \\ \alpha \cdot \|x - y\|_2 &\leq \|\varphi(x) - \varphi(y)\|_2 \leq \beta \cdot \|x - y\|_2. \end{aligned}$$

2. *Conditioning. All matrices $\{W_l\}_{l=1}^L$, $\{\tilde{W}_l\}_{l=1}^L$ and perturbations $\{\Delta W_l\}_{l=1}^L$ have condition number no larger than κ .*

Then a) for all non-zero inputs $x \in \mathbb{R}^{n_0}$, the relative functional difference obeys:

$$\frac{\|\tilde{f}(x) - f(x)\|_2}{\|f(x)\|_2} \leq \left(\frac{\beta}{\alpha} \kappa^2\right)^L \left[\prod_{k=1}^L \left(1 + \frac{\|\Delta W_k\|_F}{\|W_k\|_F}\right) - 1 \right].$$

And b) the layer- l -to-output Jacobian satisfies:

$$\frac{\left\| \frac{\partial \tilde{f}}{\partial h_l} - \frac{\partial f}{\partial h_l} \right\|_F}{\left\| \frac{\partial f}{\partial h_l} \right\|_F} \leq \left(\frac{\beta}{\alpha} \kappa^2\right)^{L-l} \left[\prod_{k=l+1}^L \frac{\beta}{\alpha} \left(1 + \frac{\|\Delta W_k\|_F}{\|W_k\|_F}\right) - 1 \right].$$

The proof is given in the appendix. The closest existing result that we are aware of is [34, Lemma 2], which bounds functional distance but not Jacobian distance. Also, since [34, Lemma 2] only holds for small perturbations, it misses the product structure of Theorem 1. It is the product structure that encodes the interactions between perturbations to different layers.

In words, Theorem 1 says that the relative change of a multilayer perceptron in terms of both function and gradient is controlled by a product over relative perturbations to each layer. Bounding the relative

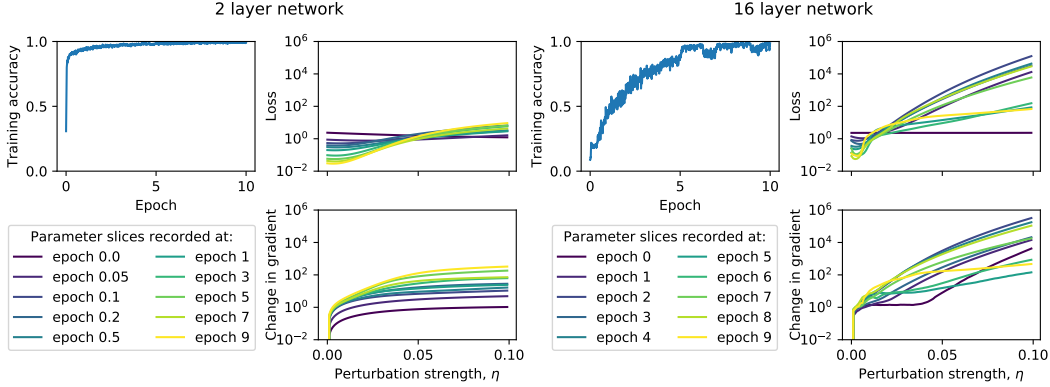


Figure 1: Using Fromage, we train a 2-layer (left) and 16-layer (right) perceptron to classify the MNIST dataset. With the network frozen at ten different training checkpoints, we first compute the gradient of the l th layer g_l using the full data batch. We then record the loss and full batch gradient \tilde{g}_l after perturbing all weight matrices W_l ($l = 1, \dots, L$) to $W_l - \eta \cdot g_l \frac{\|W_l\|_F}{\|g_l\|_F}$ for various perturbation strengths η . We plot the classification loss and the relative change in gradient of the input layer $\|\tilde{g}_1 - g_1\|_F / \|g_1\|_F$ along these parameter slices, all on a log scale. We find that the loss and relative change in gradient grow quasi-exponentially when the perceptron is deep, suggesting that Euclidean trust is violated. As such, these results are more consistent with our notion of deep relative trust.

change in function f in terms of the relative change in parameters W is reminiscent of a concept from numerical analysis known as the *relative condition number*. The relative condition number of a numerical technique measures the sensitivity of the technique to input perturbations. This suggests that we may think of Theorem 1 as establishing the relative condition number of a neural network with respect to parameter perturbations.

The two most striking consequences of Theorem 1 are that for a multilayer perceptron:

1. The trust region is not quadratic, but rather quasi-exponential at large depth L .
2. The trust region depends on the relative strength of perturbations to each layer.

To validate these theoretical consequences, Figure 1 displays the results of an empirical study. For two multilayer perceptrons of depth 2 and 16, we measured the stability of the loss and gradient to perturbation at various stages of training. For the depth 16 network, we found that the loss and gradient did breakdown quasi-exponentially in the layerwise relative size of a parameter perturbation. For the depth 2 network, the breakdown was much milder.

We will now discuss the plausibility of the assumptions made in Theorem 1. The first assumption amounts to assuming that the nonlinearity must transmit a certain fraction of its input. This is satisfied, for example, by the “leaky relu” nonlinearity, where for $0 < a \leq 1$:

$$\text{leaky_relu}(x) := \begin{cases} x & \text{if } x \geq 0; \\ ax & \text{if } x < 0. \end{cases}$$

Many nonlinearities only transmit half of their input domain—for example, the relu nonlinearity:

$$\text{relu}(x) := \max(0, x).$$

Although relu is technically not covered by Theorem 1, we may model the fact that it transmits half its input domain by setting $\alpha = \beta = \frac{1}{2}$.

The second assumption is that all weight matrices and perturbations are full rank. In general this assumption may be violated. But provided that a small amount of noise is present in the updates, then by smoothed analysis of the matrix condition number [35, 36] it may often hold in practice.

4 Descent under deep relative trust

In the last section we studied the relative functional difference and gradient difference between two neural networks. Whilst the relative breakdown in gradient is intuitively an important object for optimisation theory, to make this intuition rigorous we have derived the following lemma:

Lemma 1. *Consider a continuously differentiable function $\mathcal{L} : \mathbb{R}^n \rightarrow \mathbb{R}$ with gradient $g : \mathbb{R}^n \rightarrow \mathbb{R}^n$. Let θ measure the angle between perturbation vector ΔW and the negative gradient $-g(W)$ evaluated at parameter vector W . Then:*

$$\mathcal{L}(W + \Delta W) - \mathcal{L}(W) \leq \|g(W)\|_2 \cdot \|\Delta W\|_2 \left[-\cos \theta + \max_{t \in [0,1]} \frac{\|g(W + t\Delta W) - g(W)\|_2}{\|g(W)\|_2} \right].$$

In words, the inequality says that the change in a function due to an input perturbation is bounded by the product of three terms. The first two terms measure the size of the gradient and the size of the perturbation. The third term is a tradeoff between how aligned the perturbation is with the gradient, and how fast the gradient breaks down. Informally, the result says: *to reduce a function, follow the negative gradient until it breaks down.*

Descent is guaranteed when the bracketed term in Lemma 1 is negative. This happens when:

$$\max_{t \in [0,1]} \frac{\|g(W + t\Delta W) - g(W)\|_2}{\|g(W)\|_2} < \cos \theta. \quad (4)$$

Geometrically, this condition requires that the maximum change in gradient along the perturbation be smaller than the projection of the gradient in that direction. The simplest strategy to meet this condition is to choose $\Delta W = -\eta g(W)$ and tune the learning rate η until the lefthand side is smaller than $\cos \theta = 1$. This is what is done in practice when gradient descent is used to train neural networks.

To do better than blindly tuning the learning rate in gradient descent, we need a way to estimate the relative gradient breakdown that appears in (4). The gradient of the loss is decomposed in Equation 2—let us inspect that result. Three of the four terms involve either a network Jacobian or a subnetwork output, for which relative change is governed by Theorem 1. Since Theorem 1 governs relative change in three of the four terms in Equation 2, we propose extending it to cover the whole expression—we call this modelling assumption *deep relative trust*.

Modelling assumption 1 (Deep relative trust). *Consider a neural network with L layers and parameters $W = (W_1, W_2, \dots, W_L)$. Consider parameter perturbation $\Delta W = (\Delta W_1, \Delta W_2, \dots, \Delta W_L)$. Let vector g denote the gradient of the network loss function \mathcal{L} . Then the gradient breakdown is bounded by:*

$$\frac{\|g(W + \Delta W) - g(W)\|_2}{\|g(W)\|_2} \leq \prod_{l=1}^L \left(1 + \frac{\|\Delta W_l\|_F}{\|W_l\|_F} \right) - 1.$$

Deep relative trust applies the functional form that appears in Theorem 1 to the gradient of the loss function. As compared to Theorem 1, we have set $\alpha = \beta = \frac{1}{2}$ (a model of relu) and $\kappa = 1$ (a model of well-conditioned matrices). Another reason that deep relative trust is a *model* rather than a *theorem* is that we have neglected the $\partial \mathcal{L} / \partial f$ term in Equation 2 which depends on the choice of loss function.

Given that deep relative trust appears to penalise the relative size of perturbations to each layer, it is natural that our learning algorithm should account for this by ensuring that layerwise perturbations are bounded like $\|\Delta W_l\|_F / \|W_l\|_F \leq \eta$ for some small $\eta > 0$. The following lemma formalises this idea. As far as we are aware, this is the first descent lemma tailored to the neural network structure.

Lemma 2. *Let \mathcal{L} be a continuously differentiable loss function for a neural network of depth L that obeys deep relative trust. Consider a perturbation $\Delta W = (\Delta W_1, \Delta W_2, \dots, \Delta W_L)$ to the parameters $W = (W_1, W_2, \dots, W_L)$ with layerwise bounded relative size, meaning that $\|\Delta W_l\|_F / \|W_l\|_F \leq \eta$ for $l = 1, \dots, L$. Let θ measure the angle between ΔW and $-g(W)$. The perturbation will decrease the loss function provided that:*

$$\eta < (1 + \cos \theta)^{\frac{1}{L}} - 1.$$

The implication of Lemma 2 is that if we make a layerwise relative perturbation of strength η to a neural network, then finding a suitable value for η (to be interpreted as the learning rate) depends only on the network depth L and the perturbation angle θ . To give a concrete example, if we take a network of depth $L < 50$ and apply a layerwise relative perturbation that is sufficiently aligned with the negative gradient, say $\theta < 45^\circ$, then a learning rate of $\eta = 0.01$ will guarantee descent.

Algorithm 1 *Fromage*—a good default $\eta = 0.01$.

Input: learning rate η and matrices $\{W_l\}_{l=1}^L$
repeat
 collect gradients $\{g_l\}_{l=1}^L$
 for layer $l = 1$ **to** L **do**
 $W_l \leftarrow \frac{1}{\sqrt{1+\eta^2}} \left[W_l - \eta \cdot \frac{\|W_l\|_F}{\|g_l\|_F} \cdot g_l \right]$
 end for
until converged

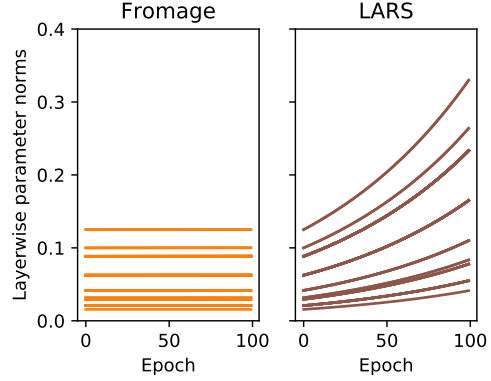


Figure 2: Left: the Fromage optimiser. Fromage differs to LARS [10] by the $1/\sqrt{1+\eta^2}$ prefactor. Right: without the prefactor, LARS suffers compounding growth in rescaling invariant layers that eventually leads to numerical overflow. This example is for a spectrally normalised cGAN [33, 37].

5 Frobenius matched gradient descent

In the previous section we established a descent lemma that takes into account the neural network structure. It is now time to apply that lemma to derive a learning algorithm.

The principle that we shall adopt is to make the largest perturbation that still guarantees descent by Lemma 2. To do this, we need to make $\cos \theta$ as large as possible whilst maintaining $\|\Delta W_l\|_F \leq \eta \|W_l\|_F$ for every layer $l = 1, \dots, L$. The simplest way to achieve this is to take the negative gradient $-g$ (for which $\cos \theta = 1$) and rescale each layer to have the proper relative size:

$$\Delta W_l = -\eta \cdot \frac{\|W_l\|_F}{\|g_l\|_F} \cdot g_l \quad \text{for } l = 1, \dots, L. \quad (5)$$

This learning rule is similar to LARS (layerwise adaptive rate scaling) proposed on empirical grounds by You et al. [10]. The authors demonstrated that LARS stabilises large batch network training.

Unfortunately, there is still an issue with this update rule that needs to be addressed. Neural network layers that involve *batch norm* [38] or *spectral norm* [33] are invariant to the rescaling map $W_l \rightarrow W_l + \alpha W_l$ and therefore the corresponding gradient g_l must lie orthogonal to W_l . This means that the learning rule in Equation 2 will increase weight norms in these layers by a constant factor every iteration. To see this, we argue by Pythagoras’ theorem combined with Equation 5:

$$\begin{aligned} & \|W_l + \Delta W_l\|_F^2 \\ &= \|W_l\|_F^2 + \|\Delta W_l\|_F^2 \\ &= (1 + \eta^2) \|W_l\|_F^2. \end{aligned}$$

This is *compounding growth* meaning that it will lead to numerical overflow if left unchecked. We empirically validate this phenomenon in Figure 2. One way to solve this problem is to introduce and tune an additional weight decay hyperparameter, and this is the strategy adopted by LARS. In this work we are seeking to dispense with unnecessary hyperparameters, and therefore we propose explicitly correcting this instability via an appropriate prefactor. We call our algorithm Frobenius matched gradient descent—or *Fromage*. See Algorithm 1 above.

The attractive feature of Algorithm 1 is that there is only one hyperparameter and its meaning is clear. Neglecting the second order correction, we have that for every layer $l = 1, \dots, L$, the algorithm’s update satisfies:

$$\frac{\|\Delta W_l\|_F}{\|W_l\|_F} = \eta. \quad (6)$$

In words: the algorithm induces a relative change of η in each layer of the neural network per iteration.

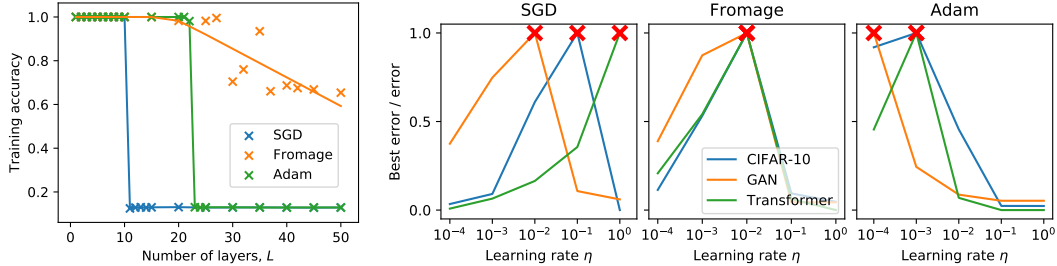


Figure 3: Left: training multilayer perceptrons at depths challenging for existing optimisers. We train multilayer perceptrons of depth L on the MNIST dataset. At each depth, we plot the training accuracy after 100 epochs. For each algorithm, we plot the best performing run over 3 learning rate settings found to be appropriate for that algorithm. We also plot trend lines to help guide the eye. Right: learning rate tuning. For each learning rate setting η , we plot the error at the best tuned η divided by the error for that η , so that a value of 1.0 corresponds to the best learning rate for that task.

Table 1: Training results. We quote loss for the classifiers, FID [4] for the GAN, and perplexity for the transformer—so lower is better. Test results and experimental details are given in Appendix C.

Benchmark	SGD η	Fromage η	Adam η	SGD	Fromage	Adam
CIFAR-10	0.1	0.01	0.001	$(1.5 \pm 0.2) \times 10^{-4}$	$(2.5 \pm 0.5) \times 10^{-5}$	$(6 \pm 3) \times 10^{-5}$
ImageNet	1.0	0.01	0.001	2.020 ± 0.003	2.001 ± 0.001	2.02 ± 0.01
GAN	0.01	0.01	0.0001	34 ± 2	16 ± 1	23.7 ± 0.7
Transformer	1.0	0.01	0.001	150.0 ± 0.3	66.1 ± 0.1	36.8 ± 0.1

6 Empirical study

To test the main prediction of our theory—that the function and gradient of a deep network break down quasi-exponentially in the size of the perturbation—we directly study the behaviour of a multilayer perceptron trained on the MNIST dataset [39] under parameter perturbations. Perturbing along the gradient direction, we find that for a deep network the change in gradient and objective function indeed grow quasi-exponentially in the relative size of a parameter perturbation (Figure 1).

The theory also predicts that the geometry of trust becomes increasingly pathological as the network gets deeper, and Fromage is specifically designed to account for this. As such, it should be easier to train very deep networks with Fromage than by using other optimisers. Testing this, we find that off-the-shelf optimisers are unable to train multilayer perceptrons (without batch norm [38] or skip connections [40]) over 25 layers deep; Fromage was able to train up to at least depth 50 (Figure 3).

Next, we benchmark Fromage on four canonical deep learning tasks: classification of CIFAR-10 & ImageNet, generative adversarial network (GAN) training on CIFAR-10, and transformer training on Wikitext-2. In theory, Fromage should be easy to use because its one hyperparameter is meaningful for neural networks and is governed by a descent lemma (Lemma 2). The results are given in Table 1. Since this paper is about optimisation, all results are reported on the training set. Test set results and full experimental details are given in Appendix C. Fromage achieved lower training error than SGD on all four tasks (and by a substantial margin on three tasks). Fromage also outperformed Adam on three out of four tasks. Most importantly, Fromage used the same learning rate $\eta = 0.01$ across all tasks. In contrast, the learning rate in SGD and Adam needed to be carefully tuned, as shown in Figure 3 (right). Note that for all algorithms, η was decayed by 10 when the loss plateaued.

7 Conclusion

We have derived a distance on deep neural networks called *deep relative trust* and used it to derive a descent lemma for neural networks. The resulting optimisation algorithm—*Fromage*—did not require learning rate grid search in any of our experiments.

Acknowledgements

The authors would like to thank Rumen Dangovski, Dillon Huff, Jeffrey Pennington, Florian Schaefer and Joel Tropp for useful conversations. They made heavy use of a codebase built by Jiahui Yu. They are grateful to Sivakumar Arayandi Thottakara, Jan Kautz, Sabu Nadarajan and Nithya Natesan for infrastructure support. JB is supported by an NVIDIA fellowship.

Broader Impact

This paper aims to improve our foundational understanding of learning in neural networks. This could lead to many unforeseen consequences down the line. An immediate practical outcome of the work is a learning rule that seems to require less hyperparameter tuning than stochastic gradient descent. This may have the following consequences:

- Network training may become less time and energy intensive.
- It may become easier to train and deploy neural networks without human oversight.
- It may become possible to train more complex network architectures to solve new problems.

In short, this paper could make a powerful tool both easier to use and easier to abuse.

References

- [1] Léon Bottou, Frank E. Curtis, and Jorge Nocedal. Optimization methods for large-scale machine learning. *SIAM Review*, 2016.
- [2] Ian Goodfellow, Yoshua Bengio, and Aaron Courville. *Deep Learning*. MIT Press, 2016. <http://www.deeplearningbook.org>.
- [3] Diederik P. Kingma and Jimmy Ba. Adam: A Method for Stochastic Optimization. In *International Conference on Learning Representations*, 2015.
- [4] Martin Heusel, Hubert Ramsauer, Thomas Unterthiner, Bernhard Nessler, and Sepp Hochreiter. GANs trained by a two time-scale update rule converge to a local Nash equilibrium. In *Neural Information Processing Systems*, 2017.
- [5] Andrew Brock, Jeff Donahue, and Karen Simonyan. Large scale GAN training for high fidelity natural image synthesis. In *International Conference on Learning Representations*, 2019.
- [6] David E. Rumelhart, Geoffrey E. Hinton, and Ronald J. Williams. Learning representations by back-propagating errors. *Nature*, 1986.
- [7] Jeffrey Pennington, Samuel Schoenholz, and Surya Ganguli. Resurrecting the sigmoid in deep learning through dynamical isometry: theory and practice. In *Neural Information Processing Systems*, 2017.
- [8] Xavier Glorot and Yoshua Bengio. Understanding the difficulty of training deep feedforward neural networks. In *International Conference on Artificial Intelligence and Statistics*, 2010.
- [9] Razvan Pascanu, Tomas Mikolov, and Yoshua Bengio. On the difficulty of training recurrent neural networks. In *International Conference on Machine Learning*, 2013.
- [10] Yang You, Igor Gitman, and Boris Ginsburg. Scaling SGD batch size to 32K for Imagenet training. Technical Report UCB/EECS-2017-156, University of California, Berkeley, 2017.
- [11] Yang You, Jing Li, Sashank Reddi, Jonathan Hseu, Sanjiv Kumar, Srinadh Bhojanapalli, Xiaodan Song, James Demmel, Kurt Keutzer, and Cho-Jui Hsieh. Large batch optimization for deep learning: Training BERT in 76 minutes. In *International Conference on Learning Representations*, 2020.
- [12] Moritz Hardt, Ben Recht, and Yoram Singer. Train faster, generalize better: Stability of stochastic gradient descent. In *International Conference on Machine Learning*, 2016.

- [13] Zeyuan Allen-Zhu. Natasha 2: Faster non-convex optimization than SGD. In *Neural Information Processing Systems*, 2018.
- [14] Simon S. Du, Chi Jin, Jason D. Lee, Michael I. Jordan, Aarti Singh, and Barnabas Poczos. Gradient descent can take exponential time to escape saddle points. In *Neural Information Processing Systems*, 2017.
- [15] Jason D. Lee, Max Simchowitz, Michael I. Jordan, and Benjamin Recht. Gradient descent only converges to minimizers. In *Conference on Learning Theory*, 2016.
- [16] Jeremy Bernstein, Yu-Xiang Wang, Kamyar Azizzadenesheli, and Animashree Anandkumar. signSGD: Compressed optimisation for non-convex problems. In *International Conference on Machine Learning*, 2018.
- [17] Florian Schaefer and Anima Anandkumar. Competitive gradient descent. In *Neural Information Processing Systems*, 2019.
- [18] Ari Benjamin, David Rolnick, and Konrad Kording. Measuring and regularizing networks in function space. In *International Conference on Learning Representations*, 2019.
- [19] Ruoyu Sun. Optimization for deep learning: theory and algorithms. *arXiv:1912.08957*, 2019.
- [20] Arkady S. Nemirovsky and David B. Yudin. *Problem complexity and method efficiency in optimization*. Wiley, 1983.
- [21] Navid Azizan and Babak Hassibi. Stochastic gradient/mirror descent: Minimax optimality and implicit regularization. In *International Conference on Learning Representations*, 2019.
- [22] Navid Azizan, Sahin Lale, and Babak Hassibi. Stochastic mirror descent on overparameterized nonlinear models: Convergence, implicit regularization, and generalization. *arXiv:1906.03830*, 2019.
- [23] Shunichi Amari. *Information geometry and its applications*. Springer, 2016.
- [24] James Martens and Roger Grosse. Optimizing neural networks with Kronecker-factored approximate curvature. In *International Conference on Machine Learning*, 2015.
- [25] Stephen Boyd and Lieven Vandenbergh. *Convex Optimization*. Cambridge University Press, 2004.
- [26] Behnam Neyshabur, Ruslan Salakhutdinov, and Nathan Srebro. Path-SGD: Path-normalized optimization in deep neural networks. In *Neural Information Processing Systems*, 2015.
- [27] Cem Anil, James Lucas, and Roger Grosse. Sorting out Lipschitz function approximation. In *International Conference on Machine Learning*, 2019.
- [28] Andrew M. Saxe, James L. McClelland, and Surya Ganguli. Exact solutions to the nonlinear dynamics of learning in deep linear neural networks. In *International Conference on Learning Representations*, 2014.
- [29] Lechao Xiao, Yasaman Bahri, Jascha Sohl-Dickstein, Samuel Schoenholz, and Jeffrey Pennington. Dynamical isometry and a mean field theory of CNNs: How to train 10,000-layer vanilla convolutional neural networks. In *International Conference on Machine Learning*, 2018.
- [30] Ge Yang and Samuel Schoenholz. Mean field residual networks: On the edge of chaos. In *Neural Information Processing Systems*, 2017.
- [31] Jeffrey Pennington and Yasaman Bahri. Geometry of neural network loss surfaces via random matrix theory. In *International Conference on Machine Learning*, 2017.
- [32] Ian Goodfellow, Jean Pouget-Abadie, Mehdi Mirza, Bing Xu, David Warde-Farley, Sherjil Ozair, Aaron Courville, and Yoshua Bengio. Generative adversarial nets. In *Neural Information Processing Systems*, 2014.

- [33] Takeru Miyato, Toshiki Kataoka, Masanori Koyama, and Yuichi Yoshida. Spectral normalization for generative adversarial networks. In *International Conference on Learning Representations*, 2018.
- [34] Behnam Neyshabur, Srinadh Bhojanapalli, and Nathan Srebro. A PAC-bayesian approach to spectrally-normalized margin bounds for neural networks. In *International Conference on Learning Representations*, 2018.
- [35] Peter Bürgisser and Felipe Cucker. Smoothed analysis of Moore-Penrose inversion. *SIAM Journal on Matrix Analysis and Applications*, 2010.
- [36] Arvind Sankar, Daniel A. Spielman, and Shang-Hua Teng. Smoothed analysis of the condition numbers and growth factors of matrices. *SIAM Journal on Matrix Analysis and Applications*, 2006.
- [37] Takeru Miyato and Masanori Koyama. cGANs with projection discriminator. In *International Conference on Learning Representations*, 2018.
- [38] Sergey Ioffe and Christian Szegedy. Batch normalization: Accelerating deep network training by reducing internal covariate shift. In *International Conference on Machine Learning*, 2015.
- [39] Yann LeCun, Leon Bottou, Yoshua Bengio, and Patrick Haffner. Gradient-based learning applied to document recognition. *Proceedings of the IEEE*, 1998.
- [40] Kaiming He, Xiangyu Zhang, Shaoqing Ren, and Jian Sun. Deep residual learning for image recognition. In *Computer Vision and Pattern Recognition*, 2016.
- [41] Alex Krizhevsky. Learning multiple layers of features from tiny images. Technical report, University of Toronto, 2009.
- [42] Christian Szegedy, Vincent Vanhoucke, Sergey Ioffe, Jon Shlens, and Zbigniew Wojna. Rethinking the Inception architecture for computer vision. In *Computer Vision and Pattern Recognition*, 2015.
- [43] Tero Karras, Timo Aila, Samuli Laine, and Jaakko Lehtinen. Progressive growing of GANs for improved quality, stability, and variation. In *International Conference on Learning Representations*, 2018.
- [44] Olga Russakovsky, Jia Deng, Hao Su, Jonathan Krause, Sanjeev Satheesh, Sean Ma, Zhiheng Huang, Andrej Karpathy, Aditya Khosla, Michael Bernstein, Alexander C. Berg, and Li Fei-Fei. ImageNet large scale visual recognition challenge. *International Journal of Computer Vision*, 2015.
- [45] Ashish Vaswani, Noam Shazeer, Niki Parmar, Jakob Uszkoreit, Llion Jones, Aidan N Gomez, Łukasz Kaiser, and Illia Polosukhin. Attention is all you need. In *Neural Information Processing Systems*, 2017.
- [46] Stephen Merity, Caiming Xiong, James Bradbury, and Richard Socher. Pointer sentinel mixture models. In *International Conference on Learning Representations*, 2017.

Appendix A A descent lemma for neural networks

Lemma 1. Consider a continuously differentiable function $\mathcal{L} : \mathbb{R}^n \rightarrow \mathbb{R}$ with gradient $g : \mathbb{R}^n \rightarrow \mathbb{R}^n$. Let θ measure the angle between perturbation vector ΔW and the negative gradient $-g(W)$ evaluated at parameter vector W . Then:

$$\mathcal{L}(W + \Delta W) - \mathcal{L}(W) \leq \|g(W)\|_2 \cdot \|\Delta W\|_2 \left[-\cos \theta + \max_{t \in [0,1]} \frac{\|g(W + t\Delta W) - g(W)\|_2}{\|g(W)\|_2} \right].$$

Proof. By the fundamental theorem of calculus,

$$\mathcal{L}(W + \Delta W) - \mathcal{L}(W) = g(W)^T \Delta W + \int_0^1 [g(W + t\Delta W) - g(W)]^T \Delta W dt.$$

The result follows by replacing the first term on the righthand side by the cosine formula for the dot product, and bounding the second term via the integral estimation lemma. \square

Lemma 2. Let \mathcal{L} be a continuously differentiable loss function for a neural network of depth L that obeys deep relative trust. Consider a perturbation $\Delta W = (\Delta W_1, \Delta W_2, \dots, \Delta W_L)$ to the parameters $W = (W_1, W_2, \dots, W_L)$ with layerwise bounded relative size, meaning that $\|\Delta W_l\|_F / \|W_l\|_F \leq \eta$ for $l = 1, \dots, L$. Let θ measure the angle between ΔW and $-g(W)$. The perturbation will decrease the loss function provided that:

$$\eta < (1 + \cos \theta)^{\frac{1}{L}} - 1.$$

Proof. Using the gradient reliability estimate from deep relative trust, we obtain that:

$$\max_{t \in [0,1]} \frac{\|g(W + t\Delta W) - g(W)\|_2}{\|g(W)\|_2} \leq \max_{t \in [0,1]} \prod_{l=1}^L \left(1 + \frac{\|t\Delta W_l\|_F}{\|W_l\|_F} \right) - 1 \leq \prod_{l=1}^L \left(1 + \frac{\|\Delta W_l\|_F}{\|W_l\|_F} \right) - 1.$$

To guarantee descent, we require that the bracketed term in Lemma 1 is negative. By the previous inequality, this will occur provided that:

$$\prod_{l=1}^L \left(1 + \frac{\|\Delta W_l\|_F}{\|W_l\|_F} \right) < 1 + \cos \theta.$$

Since $\|\Delta W_l\|_F / \|W_l\|_F \leq \eta$ for $l = 1, \dots, L$, this inequality will be satisfied provided that $(1 + \eta)^L < 1 + \cos \theta$. After a simple rearrangement, we are done. \square

Appendix B A perturbation analysis of the multilayer perceptron

We begin by fleshing out the analysis of the two-layer scalar network (Equation 3), since this example already goes a long way to exposing the relevant mathematical structure.

Consider $f : \mathbb{R} \rightarrow \mathbb{R}$ defined by $f(x) = a \cdot b \cdot x$ for $a, b \in \mathbb{R}$. Also consider perturbed function $\tilde{f}(x) = \tilde{a} \cdot \tilde{b} \cdot x$ where $\tilde{a} := a + \Delta a$ and $\tilde{b} := b + \Delta b$. The relative difference obeys:

$$\begin{aligned} \frac{|\tilde{f}(x) - f(x)|}{|f(x)|} &= \left| \frac{\tilde{a}\tilde{b}x - abx}{abx} \right| = \left| \frac{(a + \Delta a)(b + \Delta b) - ab}{ab} \right| = \left| \left(1 + \frac{\Delta a}{a}\right) \left(1 + \frac{\Delta b}{b}\right) - 1 \right| \\ &\leq \left(1 + \frac{|\Delta a|}{|a|}\right) \left(1 + \frac{|\Delta b|}{|b|}\right) - 1. \end{aligned}$$

Our main theorem will generalise this argument to more involved cases:

Theorem 1. *Let f be a multilayer perceptron with nonlinearity φ and L weight matrices $\{W_l\}_{l=1}^L$. Let \tilde{f} be a second network with the same architecture but different weight matrices $\{\tilde{W}_l\}_{l=1}^L$. For convenience, define layerwise perturbation matrices $\{\Delta W_l := \tilde{W}_l - W_l\}_{l=1}^L$.*

Further suppose that the following two conditions hold:

1. *Transmission. There exist $\alpha, \beta \geq 0$ such that $\forall x, y$:*

$$\begin{aligned} \alpha \cdot \|x\|_2 &\leq \|\varphi(x)\|_2 \leq \beta \cdot \|x\|_2; \\ \alpha \cdot \|x - y\|_2 &\leq \|\varphi(x) - \varphi(y)\|_2 \leq \beta \cdot \|x - y\|_2. \end{aligned}$$

2. *Conditioning. All matrices $\{W_l\}_{l=1}^L$, $\{\tilde{W}_l\}_{l=1}^L$ and perturbations $\{\Delta W_l\}_{l=1}^L$ have condition number no larger than κ .*

Then a) for all non-zero inputs $x \in \mathbb{R}^{n_0}$, the relative functional difference obeys:

$$\frac{\|\tilde{f}(x) - f(x)\|_2}{\|f(x)\|_2} \leq \left(\frac{\beta}{\alpha} \kappa^2\right)^L \left[\prod_{k=1}^L \left(1 + \frac{\|\Delta W_k\|_F}{\|W_k\|_F}\right) - 1 \right].$$

And b) the layer- l -to-output Jacobian satisfies:

$$\frac{\left\| \frac{\partial \tilde{f}}{\partial h_l} - \frac{\partial f}{\partial h_l} \right\|_F}{\left\| \frac{\partial f}{\partial h_l} \right\|_F} \leq \left(\frac{\beta}{\alpha} \kappa^2\right)^{L-l} \left[\prod_{k=l+1}^L \frac{\beta}{\alpha} \left(1 + \frac{\|\Delta W_k\|_F}{\|W_k\|_F}\right) - 1 \right].$$

Though we shall prove the two parts of this theorem separately, the following lemma shall help in both cases.

Lemma 3 (Relative matrix-matrix conditioning). *Consider any two matrices $\tilde{M}, M \in \mathbb{R}^{n \times m}$ with condition number bounded by κ . Then for any matrix X and any non-zero matrix Y :*

$$\frac{\|\tilde{M}X\|_F}{\|MY\|_F} \leq \kappa^2 \frac{\|\tilde{M}\|_F \|X\|_F}{\|M\|_F \|Y\|_F}.$$

Proof. Denote the singular values of M by $\sigma_1 \geq \sigma_2 \geq \dots \geq \sigma_{\bar{n}}$ and the singular values of \tilde{M} by $\tilde{\sigma}_1 \geq \tilde{\sigma}_2 \geq \dots \geq \tilde{\sigma}_{\bar{n}}$. Observe that by letting \tilde{M} and M act on the columns of X and Y (denoted x_i and y_j respectively) we have:

$$\frac{\|\tilde{M}X\|_F^2}{\|MY\|_F^2} = \frac{\sum_i \|\tilde{M}x_i\|_2^2}{\sum_j \|My_j\|_2^2} \leq \frac{\sigma_1^2 \sum_i \|x_i\|_2^2}{\tilde{\sigma}_{\bar{n}}^2 \sum_j \|y_j\|_2^2} = \frac{\tilde{\sigma}_1^2 \|X\|_F^2}{\tilde{\sigma}_{\bar{n}}^2 \|Y\|_F^2}.$$

Since for all $i = 1, \dots, \bar{n}$ it holds that $\sigma_1/\sigma_i \leq \kappa$, we obtain the following inequalities:

$$\begin{aligned} \|\tilde{M}\|_F^2 &= \sum_{i=1}^{\bar{n}} \tilde{\sigma}_i^2 \geq \tilde{\sigma}_1^2 + (\bar{n} - 1) \frac{\tilde{\sigma}_1^2}{\kappa^2} = \tilde{\sigma}_1^2 \left(1 + \frac{\bar{n} - 1}{\kappa^2}\right). \\ \|M\|_F^2 &= \sum_{i=1}^{\bar{n}} \sigma_i^2 \leq \bar{n} \sigma_1^2 \leq \bar{n} \kappa^2 \sigma_{\bar{n}}^2. \end{aligned}$$

To complete the proof, we substitute these two results into the first inequality:

$$\frac{\|\widetilde{M}X\|_F}{\|MY\|_F} \leq \frac{\widetilde{\sigma}_1 \|X\|_F}{\sigma_{\bar{n}} \|Y\|_F} \leq \frac{\sqrt{\bar{n}}\kappa}{\sqrt{1 + \frac{\bar{n}-1}{\kappa^2}}} \frac{\|\widetilde{M}\|_F \|X\|_F}{\|M\|_F \|Y\|_F} \leq \kappa^2 \frac{\|\widetilde{M}\|_F \|X\|_F}{\|M\|_F \|Y\|_F},$$

where the last inequality follows by noting that $\sqrt{\bar{n}} \leq \sqrt{\kappa^2 + \bar{n} - 1}$ since $\kappa \geq 1$. \square

With this tool in hand, let us proceed to prove part a) of Theorem 1.

Proof of Theorem 1 part a). To make an inductive argument, we shall assume that the result holds for a network with $L - 1$ layers. Extending to depth L , we have:

$$\begin{aligned} \frac{\|\widetilde{f}(x) - f(x)\|_2}{\|f(x)\|_2} &= \frac{\|(\varphi \circ \widetilde{W}_L) \circ \widetilde{h}_{L-1}(x) - (\varphi \circ W_L) \circ h_{L-1}(x)\|_2}{\|(\varphi \circ W_L) \circ h_{L-1}(x)\|_2} \\ &\leq \frac{\beta}{\alpha} \frac{\|\widetilde{W}_L \widetilde{h}_{L-1}(x) - W_L h_{L-1}(x)\|_2}{\|W_L h_{L-1}(x)\|_2} \quad (\text{assumption on } \varphi) \\ &= \frac{\beta}{\alpha} \frac{\|\Delta W_L \widetilde{h}_{L-1}(x) + W_L(\widetilde{h}_{L-1}(x) - h_{L-1}(x))\|_2}{\|W_L h_{L-1}(x)\|_2} \\ &\leq \frac{\beta}{\alpha} \frac{\|\Delta W_L \widetilde{h}_{L-1}(x)\|_2 + \|W_L(\widetilde{h}_{L-1}(x) - h_{L-1}(x))\|_2}{\|W_L h_{L-1}(x)\|_2} \quad (\text{triangle inequality}) \\ &\leq \frac{\beta}{\alpha} \kappa^2 \left[\frac{\|\Delta W_L\|_F}{\|W_L\|_F} \frac{\|\widetilde{h}_{L-1}(x)\|_2}{\|h_{L-1}(x)\|_2} + \frac{\|\widetilde{h}_{L-1}(x) - h_{L-1}(x)\|_2}{\|h_{L-1}(x)\|_2} \right]. \quad (\text{Lemma 3}) \end{aligned}$$

Whilst the second term may be bounded by the inductive hypothesis, we shall now show that the first term obeys:

$$\frac{\|\widetilde{h}_{L-1}(x)\|_2}{\|h_{L-1}(x)\|_2} \leq \left(\frac{\beta}{\alpha} \kappa^2 \right)^{L-1} \prod_{k=1}^{L-1} \left(1 + \frac{\|\Delta W_k\|_F}{\|W_k\|_F} \right).$$

We argue as follows:

$$\begin{aligned} \frac{\|\widetilde{h}_{L-1}(x)\|_2}{\|h_{L-1}(x)\|_2} &= \frac{\|\varphi(\widetilde{W}_{L-1} \widetilde{h}_{L-2}(x))\|_2}{\|\varphi(W_{L-1} h_{L-2}(x))\|_2} \\ &\leq \frac{\beta}{\alpha} \frac{\|\widetilde{W}_{L-1} \widetilde{h}_{L-2}(x)\|_2}{\|W_{L-1} h_{L-2}(x)\|_2} \quad (\text{assumption on } \varphi) \\ &\leq \frac{\beta}{\alpha} \kappa^2 \frac{\|\widetilde{W}_{L-1}\|_F}{\|W_{L-1}\|_F} \frac{\|\widetilde{h}_{L-2}(x)\|_2}{\|h_{L-2}(x)\|_2} \quad (\text{Lemma 3}) \\ &\leq \frac{\beta}{\alpha} \kappa^2 \frac{\|W_{L-1}\|_F + \|\Delta W_{L-1}\|_F}{\|W_{L-1}\|_F} \frac{\|\widetilde{h}_{L-2}(x)\|_2}{\|h_{L-2}(x)\|_2} \quad (\text{triangle inequality}) \\ &= \frac{\beta}{\alpha} \kappa^2 \left(1 + \frac{\|\Delta W_{L-1}\|_F}{\|W_{L-1}\|_F} \right) \frac{\|\widetilde{h}_{L-2}(x)\|_2}{\|h_{L-2}(x)\|_2}. \end{aligned}$$

The statement follows from an obvious induction on depth. Substituting this result and the inductive hypothesis back into the bound on $\|\widetilde{f}(x) - f(x)\|_2 / \|f(x)\|_2$, we obtain:

$$\begin{aligned} \frac{\|\widetilde{f}(x) - f(x)\|_2}{\|f(x)\|_2} &\leq \left(\frac{\beta}{\alpha} \kappa^2 \right)^L \left[\frac{\|\Delta W_L\|_F}{\|W_L\|_F} \prod_{k=1}^{L-1} \left(1 + \frac{\|\Delta W_k\|_F}{\|W_k\|_F} \right) + \prod_{k=1}^{L-1} \left(1 + \frac{\|\Delta W_k\|_F}{\|W_k\|_F} \right) - 1 \right] \\ &= \left(\frac{\beta}{\alpha} \kappa^2 \right)^L \left[\prod_{k=1}^L \left(1 + \frac{\|\Delta W_k\|_F}{\|W_k\|_F} \right) - 1 \right]. \end{aligned}$$

\square

Let us now proceed to the second part of Theorem 1.

Proof of Theorem 1 part b). By Proposition 1, the layer- l -to-output Jacobian J_l satisfies:

$$J_l := \frac{\partial f(x)}{\partial h_l} = \Phi'_L W_L \cdot \Phi'_{L-1} W_{L-1} \cdot \dots \cdot \Phi'_{l+1} W_{l+1}$$

where $\Phi'_k := \text{diag}[\varphi'(W_k h_{k-1}(x))]$. Denote the perturbed version \tilde{J}_l by the product:

$$\tilde{J}_l := \frac{\partial \tilde{f}(x)}{\partial h_l} = (\Phi'_L + \Delta\Phi'_L)(W_L + \Delta W_L) \cdot \dots \cdot (\Phi'_{l+1} + \Delta\Phi'_{l+1})(W_{l+1} + \Delta W_{l+1}).$$

For the purpose of an inductive argument, let us define the tail T_l of the Jacobian to satisfy:

$$J_l = \Phi'_L W_L T_l$$

and similarly for the perturbed version \tilde{T}_l . The inductive hypothesis then becomes:

$$\frac{\|\tilde{T}_l - T_l\|_F}{\|T_l\|_F} \leq \left(\frac{\beta}{\alpha} \kappa^2\right)^{L-l-1} \left[\prod_{k=l+1}^{L-1} \frac{\beta}{\alpha} \left(1 + \frac{\|\Delta W_k\|_F}{\|W_k\|_F}\right) - 1 \right].$$

We need to extend this to J_l . First note that by taking limits of the condition on the nonlinearity, we obtain that $0 \leq \alpha \leq \varphi'(x) \leq \beta$ for all x . This implies that for all layers l the entries of the diagonal matrix Φ'_l lie between α and β and the maximum entry of the diagonal matrix $\Delta\Phi'_l$ is no larger than $\beta - \alpha$. We shall use this information along with the triangle inequality and Lemma 3 to obtain the following:

$$\begin{aligned} \frac{\|\tilde{J}_l - J_l\|_F}{\|J_l\|_F} &= \frac{\|(\Phi'_L + \Delta\Phi'_L)(W_L + \Delta W_L)\tilde{T}_l - \Phi'_L W_L T_l\|_F}{\|\Phi'_L W_L T_l\|_F} \\ &= \frac{\|\Delta\Phi'_L(W_L + \Delta W_L)\tilde{T}_l + \Phi'_L[(W_L + \Delta W_L)\tilde{T}_l - W_L T_l]\|_F}{\|\Phi'_L W_L T_l\|_F} \\ &\leq \frac{\|\Delta\Phi'_L(W_L + \Delta W_L)\tilde{T}_l\|_F + \|\Phi'_L[(W_L + \Delta W_L)\tilde{T}_l - W_L T_l]\|_F}{\|\Phi'_L W_L T_l\|_F} \\ &\leq \frac{(\beta - \alpha)\|(W_L + \Delta W_L)\tilde{T}_l\|_F + \beta\|(W_L + \Delta W_L)\tilde{T}_l - W_L T_l\|_F}{\alpha\|W_L T_l\|_F} \\ &\leq \frac{(\beta - \alpha)\|(W_L + \Delta W_L)\tilde{T}_l\|_F + \beta\|\Delta W_L \tilde{T}_l\|_F + \beta\|W_L(\tilde{T}_l - T_l)\|_F}{\alpha\|W_L T_l\|_F} \\ &\leq \kappa^2 \frac{(\beta - \alpha)\|W_L + \Delta W_L\|_F \|\tilde{T}_l\|_F + \beta\|\Delta W_L\|_F \|\tilde{T}_l\|_F + \beta\|W_L\|_F \|\tilde{T}_l - T_l\|_F}{\alpha\|W_L\|_F \|T_l\|_F} \\ &\leq \kappa^2 \left[\frac{\beta - \alpha}{\alpha} \left(1 + \frac{\|\Delta W_L\|_F}{\|W_L\|_F}\right) \frac{\|\tilde{T}_l\|_F}{\|T_l\|_F} + \frac{\beta}{\alpha} \frac{\|\Delta W_L\|_F}{\|W_L\|_F} \frac{\|\tilde{T}_l\|_F}{\|T_l\|_F} + \frac{\beta}{\alpha} \frac{\|\tilde{T}_l - T_l\|_F}{\|T_l\|_F} \right]. \end{aligned}$$

The last term may be bounded using the inductive hypothesis, but we must still bound $\|\tilde{T}_l\|_F/\|T_l\|_F$. To economise on notation, let us construct the argument for J_l rather than T_l :

$$\frac{\|\tilde{J}_l\|_F}{\|J_l\|_F} = \frac{\|\tilde{\Phi}'_L \tilde{W}_L \tilde{T}_l\|_F}{\|\Phi'_L W_L T_l\|_F} \leq \frac{\beta \|\tilde{W}_L \tilde{T}_l\|_F}{\alpha \|W_L T_l\|_F} \leq \frac{\beta}{\alpha} \kappa^2 \frac{\|\tilde{W}_L\|_F \|\tilde{T}_l\|_F}{\|W_L\|_F \|T_l\|_F} \leq \frac{\beta}{\alpha} \kappa^2 \left(1 + \frac{\|\Delta W_L\|_F}{\|W_L\|_F}\right) \frac{\|\tilde{T}_l\|_F}{\|T_l\|_F}.$$

By a simple induction, we then obtain:

$$\frac{\|\tilde{J}_l\|_F}{\|J_l\|_F} \leq \prod_{k=l+1}^L \frac{\beta}{\alpha} \kappa^2 \left(1 + \frac{\|\Delta W_k\|_F}{\|W_k\|_F}\right) \implies \frac{\|\tilde{T}_l\|_F}{\|T_l\|_F} \leq \prod_{k=l+1}^{L-1} \frac{\beta}{\alpha} \kappa^2 \left(1 + \frac{\|\Delta W_k\|_F}{\|W_k\|_F}\right).$$

Since $\beta > \alpha$, we are free to relax the latter bound to:

$$\frac{\|\tilde{T}_l\|_F}{\|T_l\|_F} \leq \left(\frac{\beta}{\alpha} \kappa^2\right)^{L-l-1} \prod_{k=l+1}^{L-1} \frac{\beta}{\alpha} \left(1 + \frac{\|\Delta W_k\|_F}{\|W_k\|_F}\right).$$

Similarly we are free to insert one additional factor of β/α into the first term of the bound on $\|\tilde{J}_l - J_l\|_F/\|J_l\|_F$, to obtain:

$$\frac{\|\tilde{J}_l - J_l\|_F}{\|J_l\|_F} \leq \frac{\beta}{\alpha} \kappa^2 \left[\frac{\beta - \alpha}{\alpha} \left(1 + \frac{\|\Delta W_L\|_F}{\|W_L\|_F} \right) \frac{\|\tilde{T}_l\|_F}{\|T_l\|_F} + \frac{\|\Delta W_L\|_F}{\|W_L\|_F} \frac{\|\tilde{T}_l\|_F}{\|T_l\|_F} + \frac{\|\tilde{T}_l - T_l\|_F}{\|T_l\|_F} \right]$$

We now substitute in the inductive hypothesis and the bound on $\|\tilde{T}_l\|_F/\|T_l\|_F$ to obtain:

$$\begin{aligned} & \frac{\|\tilde{J}_l - J_l\|_F}{\|J_l\|_F} \\ & \leq \left(\frac{\beta}{\alpha} \kappa^2 \right)^{L-l} \left[\left[\frac{\beta - \alpha}{\alpha} \left(1 + \frac{\|\Delta W_L\|_F}{\|W_L\|_F} \right) + \frac{\|\Delta W_L\|_F}{\|W_L\|_F} + 1 \right] \prod_{k=l+1}^{L-1} \frac{\beta}{\alpha} \left(1 + \frac{\|\Delta W_k\|_F}{\|W_k\|_F} \right) - 1 \right] \\ & = \left(\frac{\beta}{\alpha} \kappa^2 \right)^{L-l} \left[\left(1 + \frac{\beta - \alpha}{\alpha} \right) \left(1 + \frac{\|\Delta W_L\|_F}{\|W_L\|_F} \right) \prod_{k=l+1}^{L-1} \frac{\beta}{\alpha} \left(1 + \frac{\|\Delta W_k\|_F}{\|W_k\|_F} \right) - 1 \right] \\ & = \left(\frac{\beta}{\alpha} \kappa^2 \right)^{L-l} \left[\prod_{k=l+1}^L \frac{\beta}{\alpha} \left(1 + \frac{\|\Delta W_k\|_F}{\|W_k\|_F} \right) - 1 \right], \end{aligned}$$

which is what needed to be shown. □

Table 2: Test set results. We quote loss for the classifiers, FID [4] for the GAN, and perplexity for the transformer—so lower is better. Training set results are given in Table 1.

Benchmark	SGD η	Fromage η	Adam η	SGD	Fromage	Adam
CIFAR-10	0.1	0.01	0.001	0.545 ± 0.002	0.31 ± 0.02	0.76 ± 0.02
ImageNet	1.0	0.01	0.001	1.091 ± 0.006	1.126 ± 0.002	1.184 ± 0.009
GAN	0.01	0.01	0.0001	34 ± 2	16 ± 1	23.9 ± 0.9
Transformer	1.0	0.01	0.0001	169.6 ± 0.6	171.1 ± 0.3	172.7 ± 0.3

Appendix C Experimental details

We provide the code used to run the experiments at <https://github.com/jxbz/fromage>. All experiments were run on a single NVIDIA Titan RTX GPU, except the ImageNet experiment which was distributed across 8 NVIDIA V100 GPUs.

We will now summarise the key details of the experimental setup.

Figure 1: measuring the loss curvature

We train multilayer perceptrons of depth 2 and 16 with relu nonlinearity on the MNIST dataset [39]. Each $28 \text{ px} \times 28 \text{ px}$ image is flattened to a 784 dimensional vector. All weight matrices of the multilayer perceptron are of dimension 784×784 , except the final output layer which is of dimension 784×10 . To train the network, we minimise the softmax cross-entropy loss function on the network output. We use the Fromage optimiser with an initial learning rate of 0.01 and reduce the learning rate by a factor of 0.9 every epoch. A training minibatch size of 250 datapoints is used. We plot the training accuracy over the 10 epochs of training, and smooth these training accuracy curves over a window length of 5 iterations to improve their legibility.

During the 10 epochs of training we record 10 snapshots of the model weights. For the 2 layer network, we record snapshots more frequently during the first epoch since this is when most of the learning happens. The 16 layer network trains slower so we record snapshots once per epoch.

For each saved snapshot of the depth $L \in \{2, 16\}$ network, we now investigate properties of the loss surface and gradient for perturbations to that snapshot. Specifically, for every layer in the network we perturb the weights W_l along the full batch gradient direction g_l . That is, for $\eta \in [0, 0.1]$ we record the loss $\mathcal{L}(\tilde{W})$ and full batch gradient \tilde{g}_l for perturbed networks with parameters given by:

$$\tilde{W}_l = W_l - \eta \cdot g_l \cdot \frac{\|W_l\|_F}{\|g_l\|_F} \quad (l = 1, \dots, L).$$

We plot the loss $\mathcal{L}(\tilde{W})$ and relative change in gradient $\frac{\|\tilde{g}_l - g_l\|_F}{\|g_l\|_F}$ for the first network layer as a function of $\eta \in [0, 0.1]$.

Figure 2 (right): stability of weight norms

With the same experimental setup as for class-conditional GAN training (see below), we run a lesion experiment on Fromage where we disable the $1/\sqrt{1 + \eta^2}$ prefactor. This makes Fromage equivalent to the LARS algorithm [10]. We plot the norms of all spectrally normalised layers in both the generator and discriminator during 100 epochs of training.

Figure 3 (left): training multilayer perceptrons at large depth

With the same basic training setup as for Figure 1, this time we vary the depth of the multilayer perceptron and benchmark SGD, Adam and Fromage. The main difference to the Figure 1 setup is that this time we train for 100 epochs (to allow more time for learning to converge) and we decay the learning rate by factor 0.95 every epoch, so that the learning rate has reduced by 2 orders of magnitude after roughly 90 epochs of training. For each learning algorithm we run three initial learning rates at each depth: for SGD we try $\eta \in \{10^0, 10^{-1}, 10^{-2}\}$, for Fromage we try $\eta \in \{10^{-1}, 10^{-2}, 10^{-3}\}$

and for Adam we try $\eta \in \{10^{-2}, 10^{-3}, 10^{-4}\}$. These values were found to be well-suited to each algorithm in preliminary experiments. For Adam we set its β_1 and β_2 hyperparameters to the standard values of 0.9 and 0.999 suggested by Kingma and Ba [3]. For SGD we set the momentum value to 0.9, and a preliminary test suggested that this improved its performance versus switching off momentum.

Figure 3 (right): learning rate tuning

For each benchmark (full details below) we conduct a learning rate grid search. For each learning rate in $\{10^{-4}, 10^{-3}, 10^{-2}, 10^{-1}, 10^0\}$ we plot the error after a fixed number of epochs. No learning rate decay schedule is used here. In the CIFAR-10 classification experiment, we record training loss at epoch 50. In the GAN experiment, we record FID between the training set and generated distribution at epoch 100. In the transformer experiment, we record training perplexity at epoch 10.

Class-conditional generative adversarial network training

We train a class-conditional generative adversarial network with projection discriminator [33, 37] on the CIFAR-10 dataset [41]. Whilst our architecture is custom, it attempts to replicate the network design of Brock et al. [5]. We use the hinge loss for training, following Miyato and Koyama [37]. We train for 120 epochs at batch size 256, and divide the learning rate by 10 at epoch 100. We make one discriminator (D) step per generator (G) step. We use equal learning rates in G and D. For all algorithms we tune the initial learning rate on a logarithmic scale (over powers of 10).

To report accuracy, we use the FID score [4]. In essence, this score measures the distance between two sets of images by measuring the difference in the first and second moments of their representations at the penultimate layer of an `inception_v3` [42] classification network. It is intended to measure a notion of *semantic distance* between two sets of images. We report the FID score between the generated distribution and both the train and test set of CIFAR-10 to provide some indication of how well the learning generalises. We do not use post-processing techniques that have been found to improve FID scores such as the *truncation trick* [5] which adjusts the input distribution to the generator at test time with a tunable hyperparameter, or by reporting FID scores on an exponential moving average of the generator [43] which also introduces an extra tunable hyperparameter.

ImageNet classification

We train the `resnet50` network [40] on the ImageNet 2012 ILSVRC dataset [44] distributed over 8 V100 GPUs. We use a batch size of 128 images per GPU, meaning that the total batch size is 1024. The network is trained for a total of 90 epochs, with the learning rate decayed by a factor of 10 after every 30 epochs. A standard data augmentation scheme is used. The initial learning rate is tuned over the set $\{10^{-3}, 10^{-2}, 10^{-1}, 10^0, 10^1\}$ based on the best top-1 accuracy on the validation subset. The final results are reported on the test subset for three runs with different random initialization seeds. For the Adam optimiser, the β_1 and β_2 parameters are set to their default values of 0.9 and 0.999 as recommended by Kingma and Ba [3]. For SGD, the weight decay coefficient is set to 10^{-4} as recommended by He et al. [40].

Wikitext-2 transformer

We train a small transformer network [45] on the Wikitext-2 dataset [46]. The code is borrowed from the Pytorch examples repository at this [https](https://github.com/pytorch/examples) url. The network is trained for 20 epochs, with the learning rate decayed by 10 at epoch 10. Perplexity is recorded on both the training and test sets. We found that without regularisation, Fromage would heavily overfit the training set. We were able to correct this behaviour by bounding each layer’s parameter norm to be smaller than its initial value.

CIFAR-10 classification

We train a `resnet18` network [40] on the CIFAR-10 dataset [41]. We train for 350 epochs and divide the learning rate by 10 at epochs 150 and 250. For data augmentation, a standard scheme is used involving random crops and horizontal flips. We report training and test loss. Again, we found that without regularisation, Fromage would heavily overfit the training set. And again, we were able to correct this behaviour by bounding each layer’s parameter norm to be smaller than its initial value.